Separation Science and Technology
Publication details, including instructions for authors and subscription information:
http://www.informaworld.com/smpp/title~content=t713708471

Soil Clean Up by in-situ Aeration. II. Effects of Impermeable Caps, Soil Permeability, and Evaporative Cooling

Keith Gannon[a]; David J. Wilson[a]; Ann N. Clarke[b]; Robert D. Mutch Jr.[b]; James H. Clarke[b]
[a] DEPARTMENT OF CHEMISTRY, VANDERBILT UNIVERSITY NASHVILLE, TENNESSEE [b] AWARE, INC. NASHVILLE, TENNESSEE

To cite this Article Gannon, Keith , Wilson, David J. , Clarke, Ann N. , Mutch Jr., Robert D. and Clarke, James H.(1989) 'Soil Clean Up by in-situ Aeration. II. Effects of Impermeable Caps, Soil Permeability, and Evaporative Cooling', Separation Science and Technology, 24: 11, 831 — 862

To link to this Article: DOI: 10.1080/01496398908049878

URL: http://dx.doi.org/10.1080/01496398908049878

SEPARATION SCIENCE AND TECHNOLOGY, 24(11), pp. 831-862, 1989

Soil Clean Up by *in-situ* Aeration. II. Effects of Impermeable Caps, Soil Permeability, and Evaporative Cooling

KEITH GANNON and DAVID J. WILSON

DEPARTMENT OF CHEMISTRY
VANDERBILT UNIVERSITY
NASHVILLE, TENNESSEE 37235

ANN N. CLARKE, ROBERT D. MUTCH JR., and JAMES H. CLARKE

AWARE, INC.
NASHVILLE, TENNESSEE 37228

Abstract

The clean up of soils contaminated by volatile compounds by *in-situ* vapor stripping was recently modeled by Wilson, Clarke, and Clarke. Their approach is modified to include the effects of a gas-impervious cap on the velocity field of the moving soil gas. Calculations indicate that such caps reduce the excessive flow of gas in the vicinity of the axis of the cylindrical volume of influence of a vent pipe, and they increase gas velocities near the periphery of the volume of influence. One thus expects use of impervious caps to improve the efficiency of *in-situ* soil vapor stripping: modeling of contaminant removal with such modified gas flow fields shows that this is indeed the case. Modeling of gas flow around buried obstacles indicates that these are not likely to interfere seriously with soil vapor stripping; some strategies are suggested to reduce their effects. The soil vapor stripping model is used to show that low soil permeabilities can be compensated for by increasing the radius of the stripping well packing. Evaporative cooling during vapor stripping is found to be insignificant under most circumstances.

INTRODUCTION

Over 1200 hazardous waste sites are currently included on EPA's National Priority List, and estimates of clean-up costs average over $10 million per site. Evidently the expenses of remediation will be quite large during the next few years, and the payoffs on improved remediation techniques could be substantial. The relatively light environmental impacts and low costs of *in-situ* methods make them quite attractive where they can be used; these methods have been reviewed by Clarke and Mutch (*1*). *In-situ* biodegradation of bydrocarbons has been described by Brubaker and Crockett (*2*). Ellis, Payne, and McNabb (*3*) and Nash (*4*) have reported on *in-situ* flushing with surfactant solutions. One of the more promising *in-situ* methods appears to be vapor stripping of volatiles (*5*).

Some excellent experimental and field work has recently been published on soil vapor stripping. Wootan and Voynick (*6*) carried out modeling experiments on the use of the technique for removing gasoline vapor from a large-scale (3 × 3 × 1.2 m) sand aquifer. They suggested that vapor stripping wells should be deep and slotted only near the bottom to avoid short-circuiting of the air flow. They also suggested that impervious covers at the surface of the vented area might improve efficiency. Both of these suggestions will be explored theoretically in the present paper.

A report from Woodward-Clyde Consultants (*7*) described a pilot soil vapor stripping study near Tacoma, Washington, and provided data strongly supporting their conclusion that the technique should be effective in remediating the site which was being tested. Anastos et al. (*8*) published the results of a pilot study of soil vapor stripping for the removal of trichloroethylene (TCE) and other volatile organics from a contaminated sandy soil at the Twin Cities Army Ammunition Plant, Minnesota. They concluded that the technology was effective, but that TCE removal from soils containing oily hydrocarbon deposits was diminished. They noted that little was known about the adsorption isotherms of the contaminants at very low concentrations. They suggested high air flow rates and close spacing of venting wells in regions of high contamination, and noted the importance of identifying these regions in the site assessment.

Crow, Anderson, and Minugh (*9*) presented data on soil vapor stripping experiments carried out at a petroleum fuels terminal at which a gasoline spill had occurred. They concluded that soil venting is effective in removing hydrocarbon vapors from the vadose zone and is also useful in augmenting conventional recovery techniques for removing spilled hydrocarbons from a shallow aquifer.

In a previous paper (*10*) we presented a mathematical model for the operation of a soil vent pipe (vapor stripping well) and showed how data could be used from lab scale aeration columns to determine parameters needed for use in the field scale vent pipe model. The soil gas velocity fields in the cylindrically shaped zone of influence around the stripping well indicated that the soil in the vicinity of the axis of the zone of influence should be cleaned up quite rapidly. The outer portions of the cylinder, through which the soil gas flows much more slowly, should be cleaned up correspondingly slowly. Calculations with the model for vapor stripping with a vent pipe bore out these surmises, and suggested that impeding the flow of gas through the surface of the soil by placing a gas-impervious circular cap on top of the soil and centered about the axis of the zone of influence should result in more effective vapor stripping.

Here we calculate the soil gas velocity field in the zone of influence around a vent pipe and examine the effects of impeding gas flow by placing gas-tight circular caps of various radii over the zone of influence of the vent pipe and centered on its axis. The notation is as in our earlier paper, the results of which will be used here without further reference (*10*). Velocity fields for both an incompressible fluid and an ideal gas were calculated; these were virtually identical, and the results of the latter calculations are presented as maps of the gas velocity vectors over a section through the zone of influence.

We then estimate the effects of impermeable obstacles in the soil on the soil gas velocity field. The presence of such obstacles (drums, metal trash, etc.) is expected to interfere with soil vapor stripping operations. We determine the streamlines of an incompressible fluid around a circular disk and around a infinite strip, both placed at right angles to an initially uniform velocity field. (Unless the percentage variation in the pressure is significant, an incompressible fluid yields a velocity field which is virtually identical to the field for an ideal gas under similar circumstances.) The times required for the fluid (gas) to move along the various streamlines are also calculated.

Out model gives expressions for the volumetric and molar flow rates through a stripping well in terms of the difference between the ambient pressure and the well head pressure, the soil permeability to gas, and the radius of the well packing. The volumetric flow rate formula is used to show that, since the flow rate depends on the product of the permeability and the packed radius of the well, a low soil permeability may be compensated for by the installation of a well with a gravel packing of large radius.

In the course of vapor stripping operations, substantial amounts of soil moisture are evaporated unless the ambient air is saturated. This might be expected to result in significant evaporative cooling of the soil, which in turn would lead to lower vapor pressures of the volatile contaminants being stripped. We therefore examine the extent to which this might be expected to occur in a representative vapor stripping situation.

FLOW FIELD FOR A COMPRESSIBLE GAS

The pressure for an ideal gas flowing through a porous medium obeys the Laplace's equation (*10*)

$$\nabla^2 P^2 = 0 \tag{1}$$

and the gas velocity is given by

$$v = -K_{\mathrm{D}} \nabla P \tag{2}$$

We consider the flow of soil gas in the vicinity of sink located at a height a above a horizontal water table or other gas-impervious layer. The surface of the soil is located at a height b above the water table, and is assumed to be horizontal, too. A circular impermeable cover of radius c is placed on the surface of the soil, centered directly over the sink which represents the vent pipe. The setup is illustrated in Fig. 1. We assume that the soil permeability is constant and isotropic. The radius of the zone of influence of the vent pipe is taken as d.

The boundary conditions for the pressure are as follows.

$$\partial P^2/\partial r = 0, r = 0, 0 \leqslant z \leqslant b, z \neq a \tag{3}$$

$$\partial P^2/\partial z = 0, 0 \leqslant r \leqslant c, z = b \tag{4}$$

$$P^2 = 1, c < r < d, z = b \tag{5}$$

$$\partial P^2/\partial r = 0, r = d, 0 \leqslant z \leqslant b \tag{6}$$

$$\partial P^2/\partial z = 0, 0 \leqslant r \leqslant d, z = 0 \tag{7}$$

The boundary operation condition given by Eq. (6) is appropriate if we assume that our zone of influence is surrounded by others identical to it;

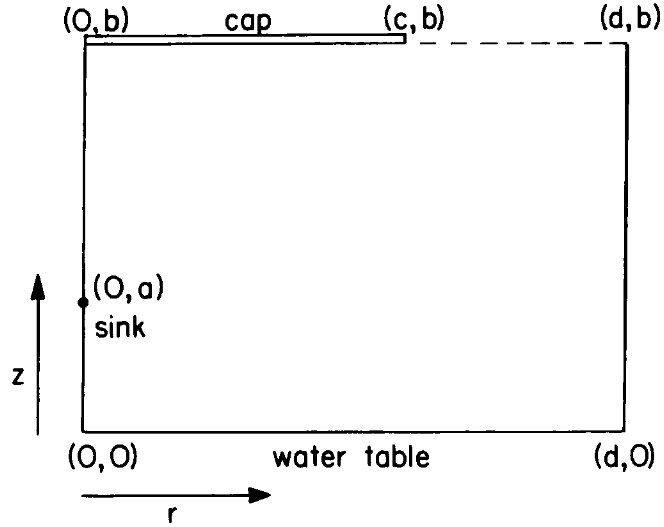

FIG. 1. The geometry of the model. The vent pipe is evacuating air from the soil at the point $(0,a)$, at a height a meters above the water table. The impervious circular cap at the surface of the ground is of radius c and is located b meters above the water table. The radius of the zone of influence is taken as d meters.

if we dealing with a single isolated vent pipe, this boundary condition should be replaced by

$$p^2 = 1 \text{ atm}^2,\ r = d,\ 0 \leqslant z \leqslant b \tag{8}$$

In either case we expect to obtain essentially the same result if d is substantially larger than both c and $b - a$ (the well depth).

We next examine what is happening in the vicinity of the sink at $(0,a)$. Let us calculate the flux of gas through the surface of a small sphere of radius ρ and centered about the point $(0,a)$. Let Q' be the flow rate (mol/s) to the sink. Then

$$Q' = \nu v_\rho c 4\pi\rho^2 \tag{9}$$

where v_ρ is the radial component of the gas velocity and c is the gas concentration at ρ, mol/m^3. From the ideal gas law,

$$c = P/RT \tag{10}$$

where P = pressure (atm)
T = temperature (°K)
R = gas constant, $8.206 \times 10^{-5}\ \mathrm{m^3 \cdot atm/mol \cdot deg}$

Also,

$$v_\rho = -K_D \frac{\partial P}{\partial \rho} \tag{11}$$

So

$$Q' = \nu K_D \frac{P}{RT} \frac{\partial P}{\partial \rho} 4\pi\rho^2 \tag{12}$$

and

$$\frac{1}{2} \frac{\partial}{\partial \rho} (P^2) = \frac{Q'RT}{4\pi\nu K_D \rho^2} \tag{13}$$

From this we obtain

$$P^2 = 1 - \frac{Q'RT}{2\pi\nu K_D \rho} \tag{14}$$

in the vicinity of the sink. Let

$$A = \frac{\pi RT}{2Q\nu K_D} \tag{15}$$

and we see that our general solution must be of the form

$$P^2 = - \frac{A}{[r^2 + (z - a)^2]^{1/2}} + u \tag{16}$$

where u is a solution of Laplace's equation which is regular at $(0,a)$ and causes P^2 to satisfy the boundary conditions, Eqs. (3)–(7).

We next rewrite these boundary conditions in terms of u; the results are as follows. u and its first derivatives are given by

$$u = P + \frac{A}{[r^2 + (z - a)^2]^{1/2}} \tag{17}$$

$$\frac{\partial u}{\partial r} = \frac{\partial P}{\partial r} - \frac{Ar}{[r^2 + (z - a)^2]^{3/2}} \tag{18}$$

$$\frac{\partial u}{\partial z} = \frac{\partial P}{\partial z} - \frac{A(z - a)}{[r^2 + (z - a)^2]^{3/2}} \tag{19}$$

The boundary conditions transform to

$$\frac{\partial u}{\partial z} = 0, r = 0, 0 \leqslant z \leqslant b \tag{20}$$

$$\frac{\partial u}{\partial z} = -\frac{A(b - a)}{[r^2 + (b - a)^2]^{3/2}} \quad, 0 \leqslant r \leqslant c, z = b \tag{21}$$

$$u = 1 + \frac{A}{[r^2 + (b - a)^2]^{1/2}} \quad, c < r \leqslant d, z = b \tag{22}$$

$$\frac{\partial u}{\partial r} = -\frac{Ad}{[d^2 + (z - a)^2]^{3/2}} \quad, r = d, 0 \leqslant z \leqslant b \tag{23}$$

$$\frac{\partial u}{\partial z} = \frac{Aa}{[r^2 + a^2]^{3/2}} \quad, 0 \leqslant r \leqslant d, z = 0 \tag{24}$$

The solution of $\nabla^2 u = 0$ for these boundary conditions given above does not appear possible by analytical methods, so numerical solution was carried out as follows. A discrete representation of Laplace's equation in cyclindrical coordinates is

$$0 = \left(1 + \frac{1}{2r_i}\right)u_{i+1,j} + \left(1 - \frac{1}{2r_i}\right)u_{i-1,j} + u_{i,j+1} + u_{i,j-1} - 4u_{ij} \tag{25}$$

where $u_{ij} = u(r_i, z_j)$
$r_i = i\Delta r$
$z_j = j\Delta z$
$\Delta z = \Delta r = 1$ unit of length

We solve this for u_{ij},

$$u_{ij} = \frac{1}{4}\left[\left(1 + \frac{1}{2r_i}\right)u_{i+1} + \left(1 - \frac{1}{2r_i}\right)u_{i-1,j} + u_{i,j+1} + u_{i,j-1}\right],$$

$$i = 1, 2, \ldots, d - 1$$

$$j = 1, 2, \ldots, b - 1 \tag{26}$$

This equation, together with discrete representations of the boundary conditions, is then used as the basis for a relaxation method of constructing the solution. One simply iterates Eqs. (26) for the interior points in the solution set and calculates the boundary points by making use of the boundary conditions after each iteration (*11*).

In the discrete representation, the boundary conditions yield the following equations:

$$u_{0,j} = u_{1,j},\ 0 \leqslant j \leqslant b \tag{27}$$

$$u_{i,b} = u_{i,b-1} - \frac{A(b-a)}{[i^2 + (b-a)^2]^{3/2}} \quad , 0 \leqslant i \leqslant c \tag{28}$$

$$u_{i,b} = 1 + \frac{A}{[i^2 + (b-c)^2]^{1/2}} \quad , c < i \leqslant d \tag{29}$$

$$u_{d,j} = u_{d-1,j} - \frac{Ad}{[d^2 + (j-a)^2]^{3/2}} \quad , 0 \leqslant j \leqslant b \tag{30}$$

$$u_{i,0} = u_{i,1} - \frac{Aa}{[i^2 + a^2]^{3/2}} \quad , 0 \leqslant i \leqslant d \tag{31}$$

We define

$$U'_{ij} = \frac{A}{[r_i^2 + (z_j - a)^2]^{1/2}} \quad , \qquad \begin{array}{l} i = 0, 1, \ldots, d \\ j = 0, 1, \ldots, b \end{array} \tag{32}$$

Then, after the u_{ij} have been calculated, the P_{ij} are given by

$$P_{ij} = [U'_{ij} + u_{ij}]^{1/2} \tag{33}$$

The velocity components of the flow field are then given at the mesh points by

$$v_r(i,j) = K_D(P_{i-1,j} - P_{i,j}) \tag{34}$$

$$v_z(i,j) = K_D(P_{i,j-1} - P_{i,j}) \tag{35}$$

The constant A, given by Eq. (15), is difficult to evaluate from this formula because of the difficulty of measuring Darcy's constant, K_D. Laboratory measurements must inevitably be flawed by disturbances of the soil resulting from taking the samples and packing them into the lab columns. We therefore next develop a computational procedure for obtaining A and K_D from readily measurable quantities. Let ρ_0 be the radius of the screened well. Recall that if f is a solution to Laplace's equation, then $\alpha f + \beta$ is also a solution, where α and β are constants. We then construct a solution f to Laplace's equation satisfying the following boundary conditions.

$$\frac{\partial f}{\partial r} = 0, r = 0, 0 \leqslant z \leqslant b \tag{36}$$

$$\frac{\partial f}{\partial z} = -\frac{(b-a)}{[r^2 + (b-a)^2]^{3/2}} \quad , 0 \leqslant r \leqslant c, z = b \tag{37}$$

$$f = \frac{1}{[r^2 + (b-a)^2]^{1/2}} \quad , c < r \leqslant d, z = b \tag{38}$$

$$\frac{\partial f}{\partial r} = -\frac{d}{[d^2 + (z-a)^2]^{3/2}} \quad , r = d, 0 \leqslant z \leqslant b \tag{39}$$

$$\frac{\partial f}{\partial z} = \frac{a}{[r^2 + a^2]^{3/2}} \quad , 0 \leqslant r \leqslant d, z = 0 \tag{40}$$

Then

$$u = Af + 1 \tag{41}$$

and

$$P^2 = -\frac{A}{[r^2 + (z - a)^2]}\frac{1}{2} + Au + 1 \tag{42}$$

At the well screen we have

$$P_w^2 = -\frac{A}{\rho_0} + Au_{I,J} + 1 \tag{43}$$

where P_w is the gas pressure (atm) in the well and the grid point (I,J) is chosen to be quite close to the location of the sink $(0,a)$. This equation is then solved for A, yielding

$$A = \frac{1 - P_w^2}{\rho_0^{-1} - u_{I,J}} \tag{44}$$

and, from Eq. (15),

$$K_D = \frac{Q'RT}{2\pi vA} \tag{45}$$

A program was written for a Zenith 151 microcomputer in BASICA; this program was run in TurboBASIC with an 8087 math coprocessor. Velocity fields were calculated for a = 3.5 m (height of well above the water table), b = 20 m (depth of water table), d = 30 m (radius of zone of influence), and c = 1, 5, 10, 15, 20, and 25 m. The screened well radius is 0.12 m, the gas flow rate is 10 mol/s in the absence of a cap, the Darcy's constant is 6.54 $m^2/atm \cdot s$, the soil voids fraction is 0.2, and the velocity magnification factor is 5×10^4. Each run took approximately half an hour. Velocity fields for runs having c = 1, 15, and 25 m are shown in Figs. 2, 3, and 4.

One is obstructing the gas flow somewhat by the use of these circular caps, and this is expected to decrease the efficiency of the vapor stripping process somewhat. However, the appearances of all the velocity fields (Figs. 2–4) indicate that the gas velocities are very much higher in the vicinity of the sink than they are anywhere else, and that therefore the bulk of the pressure drop occurs in the vicinity of the sink. This leads one to conclude that changes made in the flow pattern through an obstacle placed some distance from the sink are unlikely to decrease the overall flow rate appreciably. The gas flow rates in the runs plotted in Figs. 2–4

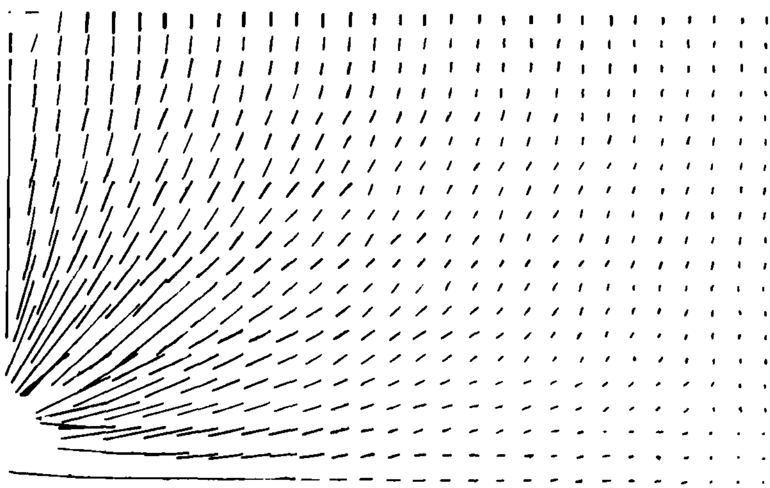

FIG. 2. Velocity field for an ideal gas. Here and in Figs. 3 and 4, temperature = 298 K, the screened radius of the well = 0.12 m, the gas pressure in the well = 0.866 atm, and the soil voids fraction = 0.2. A similar run with no cap and a gas flow rate of 10 mol/s yielded K_D = 6.54 m^2/atm · s, which was then used in Figs. 2, 3, and 4. The radius of the impervious cap = 1 m, and Q is found to be 9.9999 mol/s.

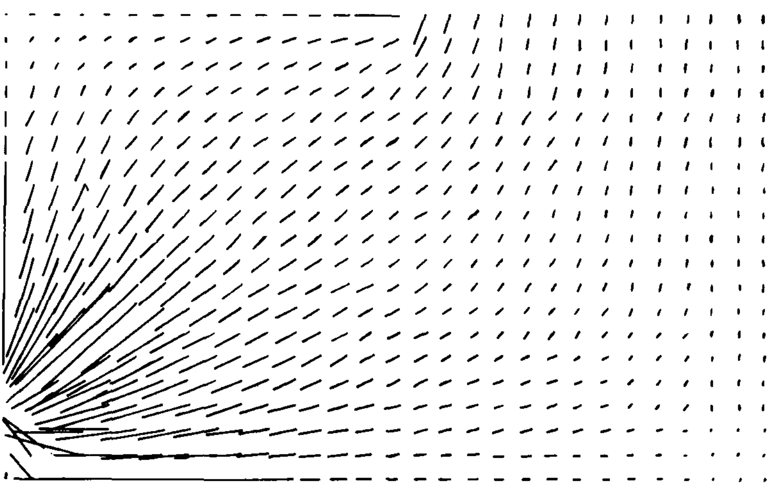

FIG. 3. Velocity field for an ideal gas. All parameters are as in Fig. 2, except that the cap radius = 15 m. The resulting gas flow rate is 9.9689 mol/s.

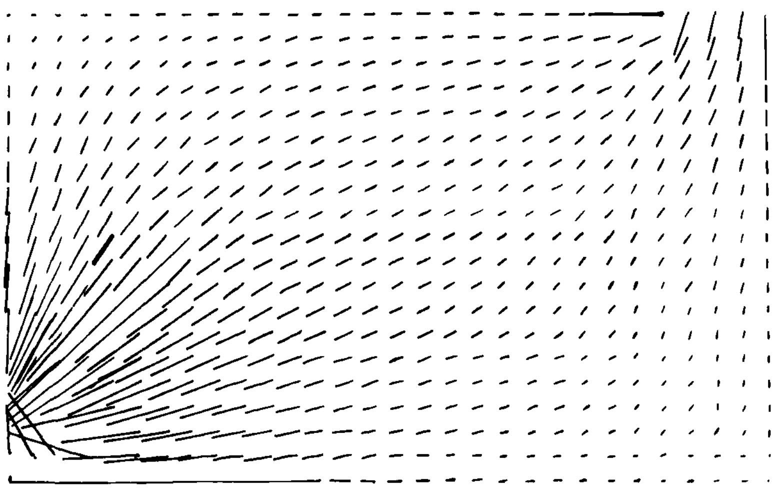

FIG. 4. Velocity field for an ideal gas. All parameters are as in Fig. 2, except that the cap radius = 25 m. The resulting gas flow rate is 9.8862 mol/s.

and several other runs show that this is indeed the case. In all these runs the Darcy's constant was 6.54 $m^2/atm \cdot s$, the value found when a flow rate of 10 mol/s was used for a run with no impervious cap. As seen in Table 1, there is a reduction in the flow rate with increasing circular cap radius, but it is quite small. With a 30-m radius of influence and a cap of radius 25 m, the flow rate is decreased by only 1.14% below its value in the absence of a cap. Evidently one can neglect the reduction in flow rate resulting from the cap for all practical purposes.

TABLE 1
Gas Flow Rates for Various Cap Diameters

Cap diameter (m)	Gas flow rate (mol/s)
0	10.0000
1	9.9999
5	9.9972
10	9.9869
15	9.9689
20	9.9406
25	9.8862

Our results for gas velocity flow fields about a vapor stripping well lead to the following conclusions. First, for the parameters used here, there is relatively little difference between the behavior of the incompressible gas model (data not shown here) and the compressible gas model. This is presumably due to the relatively small pressure drop in the well (wellhead pressure = 0.866 atm). Second, use of a circular cap causes substantial increases in gas velocities in the peripheral regions of the zone of influence, and can therefore be expected to reduce the times required for remediation by *in-situ* soil vapor stripping. Third, the velocity fields calculated for small circular caps by the relaxation method used here appear to be virtually identical to those calculated by the method of images for systems without impervious caps (*10*); this gives one increased confidence in both sets of results. Fourth, use of these soil gas velocity fields in the modeling of *in-situ* soil vapor stripping should be no more difficult than use of soil gas velocity fields calculated by the method of images and employed in our earlier work. Fifth, the use of impervious caps to improve gas flow patterns decreases gas flow rates negligibly. This also suggests that the presence of paved streets, parking lots, building floors, etc. may not interfere significantly with a properly designed vapor stripping system.

FLOW FIELDS AROUND OBSTACLES IN THE SOIL

We next address the effects of impermeable obstacles in the soil on the soil gas velocity field. The presence of buried drums and other scrap will certainly reduce the efficiency of soil vapor stripping operations. One can conceive of obstacle shapes which would result in soil pockets from which vapor stripping would be extremely slow; soil contained in a drum open at one end, for instance.

Here we examine the streamlines and transit times of soil gas moving in an initially uniform flow field into which we place either an impermeable horizontal strip of width $2a$ and infinite length, or an impermeable horizontal disk of radius a. The geometry is shown in Fig. 5. We assume that the pressure drop in the domain of interest is small enough so that the gas may be regarded as incompressible.

As before, the velocity of the soil gas is given by

$$v = -K_D \nabla P \tag{2}$$

and we assume that the pressure satisfies Laplace's equation when the flow is independent of time (steady state).

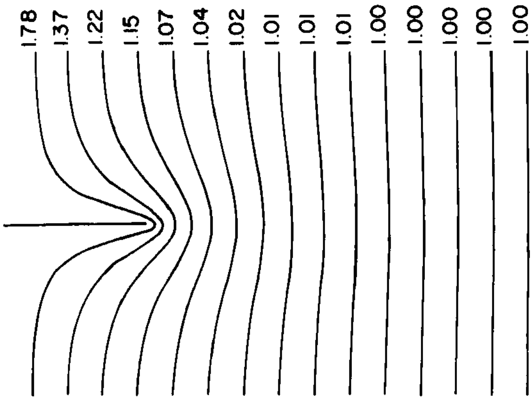

FIG. 5. Gas streamlines and relative transit times around an infinitely long strip of 40 cm width. The region mapped is 80 × 80 cm in this and the next two figures. The gas is assumed to be incompressible.

$$\nabla^2 P = 0 \tag{46}$$

Consider the case of a horizontal impermeable strip of width $2a$ and infinite length. For this case

$$\frac{\partial^2 P}{\partial x^2} + \frac{\partial^2 P}{\partial z^2} = 0 \tag{47}$$

with boundary conditions

$$P = 1, z = 0, 0 < x < 80 \text{ cm} \tag{48}$$

$$P = 0, z = 80, 0 < x < 80 \tag{49}$$

$$\partial P/\partial x = 0, x = \ , 0 < z < 80 \tag{50}$$

$$\partial P/\partial x = 0, x = 80, 0 < z < 80 \tag{51}$$

$$\partial P/\partial z = 0, z = 40 - \delta, 0 < x < a \tag{52}$$

$$\partial P/\partial z = 0, z = 40 + \delta, 0 < x < a \tag{53}$$

Equations (52) and (53) introduce the impermeable obstacle. Equation (50) is due to the symmetry of the problem. Equation (51) introduces the assumption that the flow on the right side is essentially unperturbed—or that there is another obstacle on the right, symmetrically placed. Equations (48) and (49) give us a constant pressure gradient (and a uniform velocity field) in the absence of an obstacle.

Equation (46) is solved by a relaxation method. We set $\Delta x = \Delta z = 1$ cm, and approximate Eq. (46) by

$$P_{ij} = \tfrac{1}{4}(P_{i-1,j} + P_{i+1,j} + P_{i,j-1} + P_{i,j+1}) \tag{54}$$

The boundary conditions are also rewritten in terms of finite differences; for instance, Eq. (51) yields

$$P_{80,j} = \tfrac{1}{3}(P_{79,j} + P_{80,j-1} + P_{80,j+1}),\ j = 2, \ldots, 79 \tag{55}$$

and Eq. (6) yields

$$P_{i,40} = \tfrac{1}{3}(P_{i,39} + P_{i+1,40} + P_{i-1,40}),\ i = 2, \ldots, a \tag{56}$$

etc.

This system of equations was then solved by relaxation, simply iterating the equations until the values of the pressures ceased to change. The soil gas velocities were then calculated from

$$v_x = -K_D \frac{\partial P}{\partial x} \tag{57}$$

$$v_z = -K_D \frac{\partial P}{\partial z} \tag{58}$$

The derivatives were calculated from a second-order Taylor's series expansion for P about the point $x_i = i\Delta x$, $z_j = j\Delta z$,

$$P(x,z) = P_{ij} + \frac{P_{i+1,j} - P_{i-1,j}}{2\Delta x}(x - i\Delta x) + \frac{P_{i,j+1} - P_{i,j-1}}{2\Delta z}(z - j\Delta z)$$

$$+ \frac{P_{i+1,j} - 2P_{ij} + P_{i-1,j}}{2\Delta x^2}(x - i\Delta x)^2$$

$$+\frac{P_{i,j+1} - 2P_{ij} + P_{i,j-1}}{2(\Delta z)^2}(z - j\,\Delta z)^2$$

$$+\frac{P_{i+1,j+1} - P_{i-1,j+1} - P_{i+1,j-1} + P_{i-1,j-1}}{4\Delta x\Delta z}(x - i\Delta x)(z - j\,\Delta z) \tag{59}$$

Differentiating with respect to x yields

$$\frac{\partial P}{\partial x} = \frac{P_{i+1,j} - P_{i-1,j}}{2\Delta x} + \frac{P_{i+1,j} - 2P_{ij} + P_{i-1,j}}{\Delta x^2}(x - i\Delta x)$$

$$+\frac{P_{i+1,j+1} - P_{i-1,j+1} - P_{i+1,j-1} + P_{i-1,j-1}}{4\Delta x\Delta z}(z - j\,\Delta z) \tag{60}$$

Similarly,

$$\frac{\partial P}{\partial z} = \frac{P_{i,j+1} - P_{i,j-1}}{2\Delta x} + \frac{P_{i,j+1} - 2P_{ij} + P_{i,j-1}}{\Delta z^2}(z - j\,\Delta z)$$

$$+\frac{P_{i+1,j+1} - P_{i-1,j+1} - P_{i+1,j-1} + P_{i-1,j-1}}{4\Delta x\Delta z}(x - i\Delta x) \tag{61}$$

These equations are used over the range $(i - ½)\Delta x < x < (i + ½)\Delta x$, $(j - ½)\Delta z < z < (j + ½)\Delta z$.

To get the streamlines of the soil gas, one then simply integrates the equations

$$\frac{dx}{dt} = -K_{\mathrm{D}}\frac{\partial P}{\partial x} \tag{62}$$

$$\frac{dz}{dt} = -K_{\mathrm{D}}\frac{\partial P}{\partial z} \tag{63}$$

numerically. Rates of gas movement along any streamline are readily determined by counting the number of time increments in the numerical integration which are required to trace out the streamline. In this way one can get some idea of the volume of soil through which the soil gas movement is seriously impeded by the obstacle.

Gas flow past a circular disk at right angles to the direction of undisturbed gas flow is also readily determined. One uses virtually the same approach as that used above for the infinite strip, except that the calculation is done in cylindrical coordinates. Laplace's equation is

$$\frac{1}{r}\frac{\partial}{\partial r}\left(r\frac{\partial P}{\partial r}\right) + \frac{\partial^2 P}{\partial z^2} = 0 \tag{64}$$

The discrete representation we used is

$$\frac{1}{\Delta r^2}\left[P_{i+1,j} - 2P_{i,j} + P_{i-1,j} + \frac{1}{2i-1}(P_{i+1,j} - P_{i-1,j})\right] + \frac{1}{\Delta z^2}[P_{i,j+1} - 2P_{i,j} + P_{i,j-1}] = 0 \tag{65}$$

This set of equations was also solved by solving for $P_{i,j}$ and then simply iterating until convergence occurred. The boundary conditions were handled very similarly to the infinite strip case.

The relaxation method converged in all the cases we tried, and the results were physically as expected, but the method is slow. Three to 6 h of machine time were required per run on an AT clone using an 80287 math chip, operating at 10 MHz, and in TurboBASIC. If one had many of these computations to do, one would be well advised to seek a more complex but faster method.

The results for infinite strips of width 20, 40, 60, and 80 cm are shown in Figs. 5-7. The number by each streamline gives the relative time required for the streamline to be traced out. In all cases half of the domain is shown, since the other half of the domain is just a mirror image. The presence of the obstruction definitely impedes gas flow for those streamlines near the center of the obstruction, but the volumes in which gas transit times are 4 times or more larger than the unimpeded transit times are relatively small. We therefore conclude that the presence of such obstacles to gas flow is not likely to seriously impede soil vapor stripping operations unless the obstacles are in a region in the zone of influence around the well where gas flow is quite slow. This would be out near the outer boundary of a zone of influence of radius somewhat larger than the depth of the well. If one knows where the obstructions are, one should place the well near the obstructions, with the well opening below them. If the obstructions are more or less randomly distributed or their location is not known, then one should space the vapor stripping wells

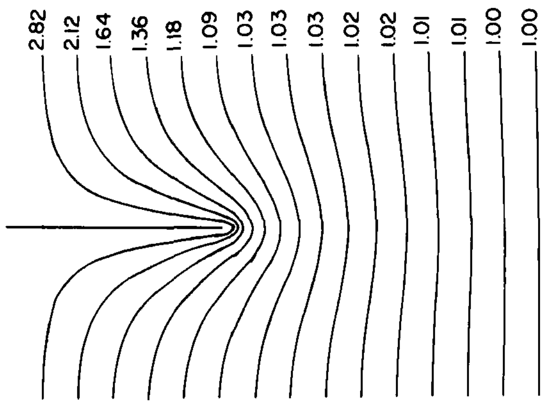

FIG. 6. Gas streamlines and relative transit times around an infinitely long strip of 60 cm width.

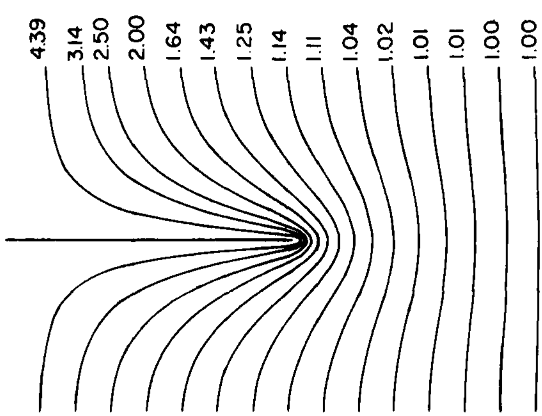

FIG. 7. Gas streamlines and relative transit times around an infinitely long strip of 80 cm width.

such that the radius of each zone of influence is somewhat less than the depth of that well, and the wells should be drilled down to as close to the water table as possible.

One note of caution. If volatile contaminants are actually enclosed or partially enclosed in an impermeable container (an buried open drum or bucket, etc.), the rate of removal of these will be very slow or essentially nil, and excavation of these pockets will be necessary.

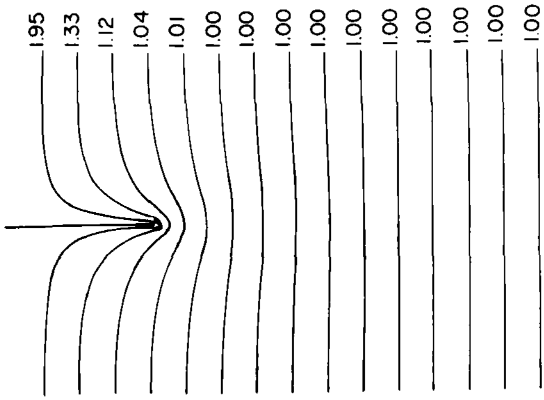

FIG. 8. Gas streamlines and relative transit times around a circular disk of 40 cm diameter.

The flow fields around a disk-shaped obstacle at right angles to the direction of flow are shown in Figs. 8–10 for disks of diameter 40, 60, and 80 cm, respectively. The numbers by the streamlines represent the time required for gas to move from 40 cm below the obstacle to 40 cm above it relative to the time required for unperturbed flow. The region in the

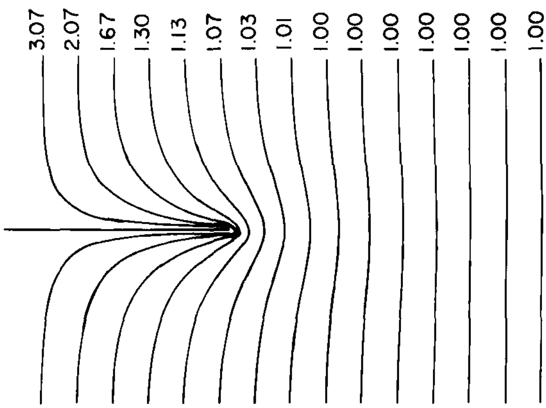

FIG. 9. Gas streamlines and relative transit times aroun da circular disk of 60 cm diameter.

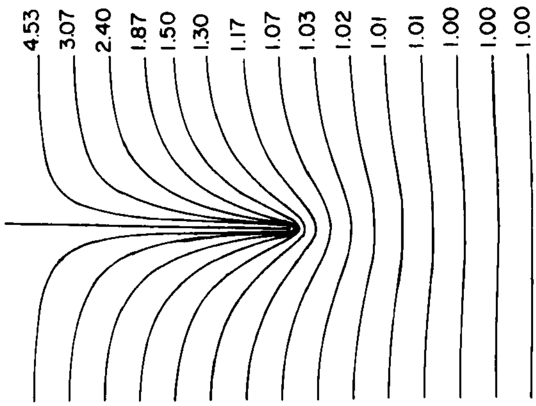

FIG. 10. Gas streamlines and relative transit times around a circular disk of 80 cm diameter.

vicinity of the obstacle in which gas transit times are increased by a factor of 4 or more is even smaller than was found with the long strip obstacles. We conclude that the results found for the circular disk obstacles change none of our previous conclusions.

VAPOR STRIPPING

The gas velocity fields calculated for wells with impermeable circular caps were used in the vapor stripping model described earlier (*10*). This model assumes that the moving vapor is in local equilibrium with the stationary liquid phase, and that one may use Henry's law to describe the partitioning of volatile solute between the stationary (liquid or absorbed) phase and the mobile vapor phase. Programs were written in TurboBASIC implementing the model. The velocity field is calculated separately and stored for use in the program which models vapor stripping. Runs were made on a MMG 286 microcomputer (an AT clone) operating at 10 MHz and using an 80287 math coprocessor. A typical run took about an hour of machine time.

We next examine some results of calculations with the soil vapor stripping model which give insight into the factors affecting contaminant removal rates. The boundary condition on the gas velocity on the outer surface of the cylindrical zone of influence, $v_r = 0$, should be a quite good

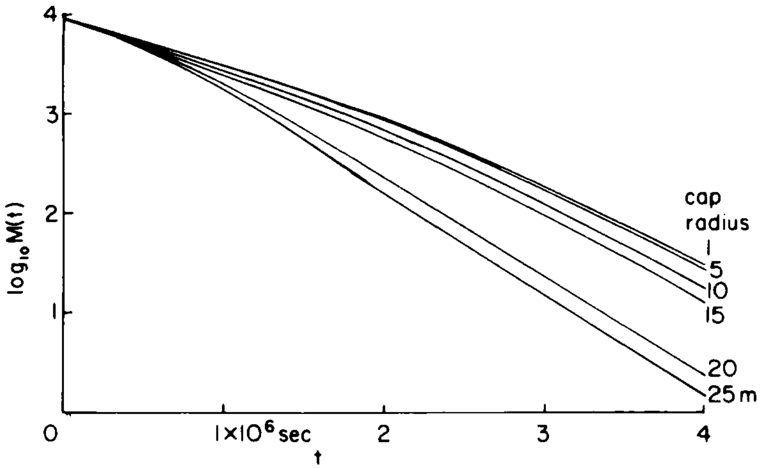

FIG. 11. Plots of $\log_{10}$ total solute mass versus time, showing the effects of circular impermeable caps on soil vapor stripping efficiency. Cap radii = 1, 5, 10, 15, 20, and 25 m. Radius of zone of influence = 30 m; depth of water table = 20 m; height of well above water table = 3 m; gas flow rate = 9.1 mol/s; Henry's constant = 0.01; well radius = 12 m; voids fraction = 0.2; soil moisture fraction = 0.2; well pressure = 0.866 atm; K_D = 6 m^2/atm · s; soil density = 1.6 g/cm^3; initial volatile solute concentration = 100 mg/kg. Three-point second-order algorithms were used to fit the boundary conditions.

approximation to that for the zone of influence of a well surrounded by six neighboring wells in a hexagonal array.

The effect of the circular impermeable caps on the removal of a volatile contaminant is shown in Fig. 11. Here the $\log_{10}$ of the total mass of contaminant remaining in the zone of influence is plotted as a function of the time. The radius of the zone of influence is 30 m, and the other model parameters are given in the caption. For this system we see that use of an impermeable cap of 25 m radius decreases the time required to achieve 99% removal to 65% of its value when a cap is not used. The radius of the zone of influence of the system described in Fig. 12 is 20 m, and the other parameters are as in Fig. 11. The advantage of using an impermeable cap is reduced somewhat when the vapor stripping wells are closer together, as is seen by comparing Figs. 11 and 12.

The influence of the spacing of the wells (which determines the radius of influence) is seen in Fig. 13. In these runs no cap was used. The water table is at a depth of 20 m and the bottom of the well is 3 m above the water table in all these runs. Evidently one pays a heavy price for spacing

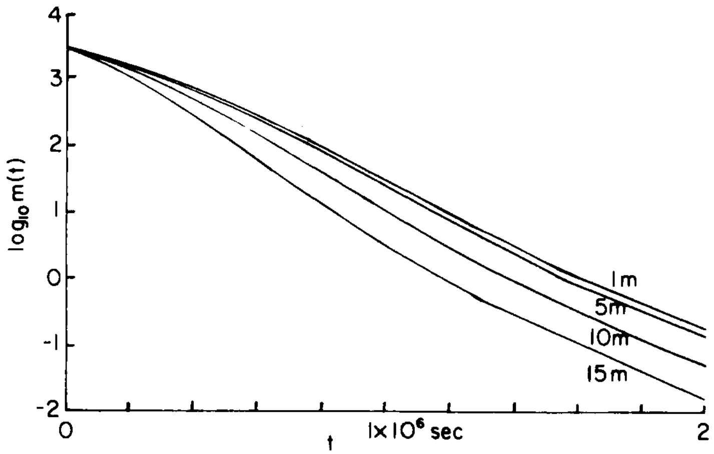

FIG. 12. Plots of $\log_{10}$ total solute mass versus time, showing the effects of impermeable cap radius on removal efficiency. Depth of water table = 15 m; radius of zone influence = 20 m; other parameters as in Fig. 11. Cap radii = 1, 5, 10, and 15 m.

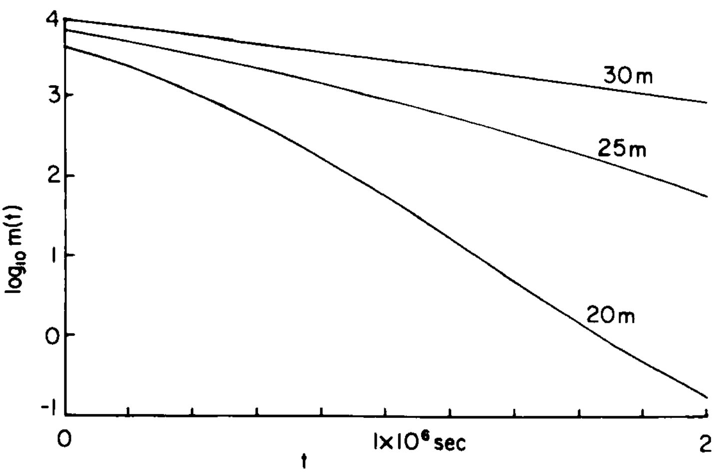

FIG. 13. Plots of $\log_{10}$ total solute mass versus time, showing the effects of well spacing on the rate of removal. No cap was used in these runs. Depth of water table = 20 m; height of well above water table = 3 m; radius of zone of influence = 20, 25, and 30 m. Other parameters as in Fig. 11.

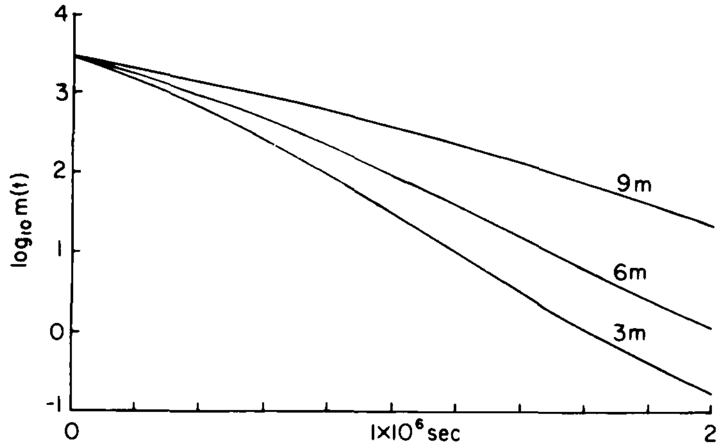

FIG. 14. Plots of $\log_{10}$ total solute mass time showing the effect of well depth. Depth of water table = 15 m; radius of zone of influence = 20 m; height of well above water table = 3, 6, and 9 m. Other parameters as in Fig. 11. No impermeable cap was used in these runs.

one's vapor stripping wells too far apart, in that the time required for clean up increases dramatically as the radius of the zone of influence increases to values substantially larger than the depth of the water table.

In our earlier paper (*10*) it was shown that more efficient vapor stripping is obtained if the bottom of the well is near the water table. If the bottom of the well is not near the water table, gas flow through that portion of the zone of influence near the axis of the zone of influence is very rapid, but gas flow through the more peripheral portions becomes extremely slow. Figure 14 shows this effect when no cap is used. Here the water table is 15 m below the surface and the radius of the zone of influence is 20 m. Raising the bottom of the well from 3 to 9 m above the water table decreases the removal rate by about 50%. The results exhibited in Fig. 15 pertain to an identical system, except that a cap of 15 m radius has been installed. The shallow well for this case has a removal rate about 33% lower than the deep well, indicating that the presence of a cap reduces somewhat the damage resulting from using shallow wells.

We also explored the effects of numerical dispersion on the soil vapor stripping model (*12*). This was done by replacing the simple algorithm we used earlier (*10*) to model advection by a substantially more elaborate algorithm which has much lower numerical dispersion. These so-called

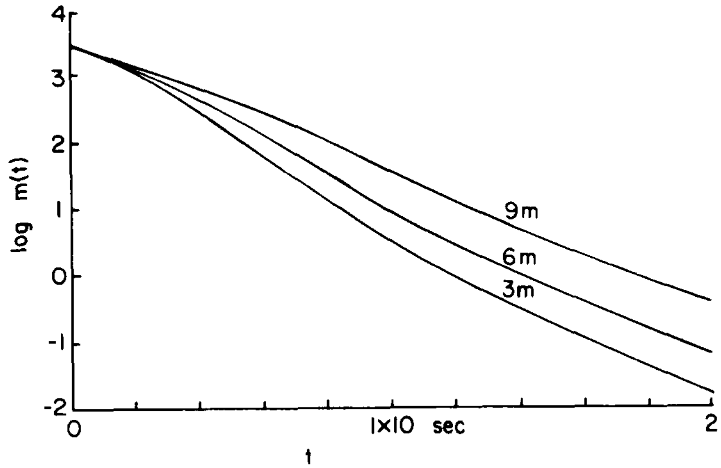

FIG. 15. Plots of $\log_{10}$ total solute mass versus time, showing the effect of well depth. Parameters are as in Fig. 14, except that an impermeable cap of 15 m radius was used.

asymmetrical upwind algorithms have been examined in detail by Leonard (*13*) and, in situations where numerical dispersion from the advection term is a problem, yield very markedly improved results.

We found, however, that comparison of the two models indicated that numerical dispersion does not appear to significantly distort the shapes of the contaminant removal curves, and that it is apparently not necessary to go to the extra effort of using these elaborate advection algorithms in soil vapor stripping models. The uncertainties in the experimental values of the parameters which are generally available for the modeling are very much greater than the differences in the results obtained with the two models. The reason for this relatively small effect is probably as follows. The gas velocities vary enormously from place to place within the zone of influence of the vapor stripping well. Even as one moves along a single gas flow streamline, the gas velocity varies greatly. Apparently the dispersive effects of these highly variable (in space) gas velocities are so large that they simply swamp out the effects of numerical dispersion. Gannon (*12*) has presented computations and a detailed discussion of these points.

COMPENSATION FOR LOW SOIL PERMEABILITY

Soil vapor stripping technique requires that the soil be sufficiently permeable to air to permit the passage of air at a reasonable rate through the soil being treated. We recall Eq. (31) from our earlier paper (*10*), which is used to calculate Darcy's constant from readily observable quantities,

$$K_D = \frac{QRT}{2\pi \nu r_s (P_a^2 - P_f^2)} \tag{66}$$

where Q = molar air flow rate
ν = soil voids fraction
P_a = ambient pressure, 1 atm
P_f = pressure inside the well, <1 atm
r_s = packed radius of the well (radius of the gravel packing around the screened bottom of the well)

This equation, derived for a velocity potential constructed by the method of images, indicates that the gas flow rate is given by

$$Q' = 2\pi \nu (P_a^2 - P_f^2) r_s K_D / RT \tag{67}$$

From this we see that one may compensate for a soil of lower permeability simply by increasing the radius of the gravel packing at the bottom of the well.

We were interested to see whether our numerical solutions to Laplace's equation yielded similar results. Several runs were made with different values of r_s and K_D, and the flow rates for these were calculated by the procedure described in the section on velocity fields. The results are shown in Table 2, and indicate that this model also yields the result that the air flow rate is directly proportional to both K_D and r_s to a very good approximation. In these runs an impermeable cap of 15 m radius was used. The other parameters are given in the table. It is thus possible, within limits, to counterbalance the effect of a low soil permeability by constructing a well with a gravel packing of large diameter. This allows one to extend the vapor stripping technique to soils of lower permeability without increasing the cost to any appreciable extent. Note, however, that in any case the well casing itself must be tightly sealed into the soil to

TABLE 2
Effects of Well Radius and K_D on Gas Flow Rates[a]

Well radius (m)	K_D (m^2/atm · s)	Molar air flow rate (mol/s)
0.12	6	9.076
0.24	3	8.905
0.24	6	17.864
0.12	3	4.543
0.36	2	8.999
0.72	1	8.760

[a]Well depth = 15 m, cap radius = 15 m, radius of zone of influence = 20 m, well is 3 m above the water table. T = 298 K, voids fraction = 0.2, well pressure = 0.866 atm.

avoid short-circuiting of air to the bottom of the well, with corresponding loss of efficiency.

SOIL TEMPERATURES

The vapor pressures of volatile contaminants depend strongly on temperature. If moist soils are vapor stripped with air that has a relative humidity of less than 100%, there may be sufficient evaporative cooling to decrease substantially the vapor pressure of the volatile contaminant(s). This would decrease removal rates by soil vapor stripping. In this section we present a calculation exploring this point.

Let v_s = volume of soil sample to be vapor stripped
c_s = specific heat of soil, cal/g · degree
l = latent heat of vaporization of water, 540 cal/g
$(7/2)R_c$ = molar heat capacity of air, cal/mol · degree (R_c = 1.987 cal/mol · degree)
$x(T)$ = relative humidity of air/100% at temperature T
dV_a = volume of air passed through soil sample
T_a = initial air temperature, °K
T_s = initial soil temperature
$T_s + dT_s$ = final soil temperature
$P_w(T_s)$ = vapor pressure of water at temperature T_s, atm
R = 82.06 mL · atm/mol · degree
ρ_s = soil density, g/mL

The basis for the calculation is the heat balance

Heat gained by air + heat gained by soil

+ heat gained by evaporated water = 0

The mass of water evaporated by a volume dV_a of air is determined as follows. From the ideal gas law, and with the assumption that the air evaporates enough water to become completely saturated, we have

$$(1 - x)P_w(T_s)dV_a = dn_wRT_s \tag{68}$$

where

$$dn_w = \text{moles of water evaporated}$$

This gives

$$dm_w = 18\,\frac{P_w(T_s)}{RT_s}\,[1 - x(T_s)]dV_a \tag{69}$$

where dm_w is the mass of water evaporated by a volume dV_a of air and 18 g/mol is the molecular weight of water. The heat absorbed by the water in evaporating is given by

$$q_{evap} = \frac{l \cdot 18 \cdot P_w(T_s)dV_a}{RT_s}\,[1 - x(T_s)] \tag{70}$$

The heat gained by the air is calculated as follows. The number of moles of air dn_a passed in a volume dV_a is given by

$$PdV_a = dn_aRT_a$$

from which we find that the heat gained by the air is

$$\delta q_{air} = \frac{7}{2}R_c\,\frac{PdV_a}{RT_a}(T_s + dT_s - T_a) \tag{71}$$

The heat gained by the soil is given by

$$\delta q_{soil} = \rho_sV_sc_sdT_s \tag{72}$$

The heat balance $\delta q_{air} + \delta q_{evap} + \delta q_{soil} = 0$ then yields

$$\frac{7}{2}R_c\frac{P(T_s - T_a)dV_a}{RT_a} + \frac{l \cdot 18 \cdot P_w(T_s)}{RT_s}[1 - x(T_s)]dV_a + P_sV_sc_sdT_s = 0 \tag{73}$$

This can be rearranged to give a differential equation for the soil temperature,

$$\frac{dT_s}{dV_a} = -\frac{1}{\rho V_sc_s}\left[\frac{7R_c \cdot 1\text{ atm} \cdot (T_s - T_a)}{2RT_a} + \frac{18lP_w(T_s)}{RT_s}[1 - x(T_s)]\right] \tag{74}$$

An excellent approximation for $P_w(T_s)$ is given by

$$P_w(T_s) = A\exp[-18l/R_cT_s] \tag{75}$$

so that

$$\frac{dT_s}{dV_a} = -\frac{1}{\rho_sV_sc_s}\left[\frac{7}{2}R_c\frac{1\text{ atm} \cdot (T_s - T_a)}{RT_a} + \frac{18l[1 - x(T_s)]}{RT_s} \times A\exp(-18l/R_cT_s)\right] \tag{76}$$

Note that if the relative humidity of the air is 100% and $T_s = T_a$, then $dT_s/dV_a = 0$, as expected. A steady-state soil temperature (good as long as there is soil moisture available) can be obtained by solving the equation

$$0 = \frac{7}{2}\frac{R_c \cdot 1\text{ atm}}{RT_a}(T_s - T_a) + \frac{18l[1 - x(T_s)]}{RT_s}A\exp\left(-\frac{18l}{R_cT_s}\right) \tag{77}$$

for T_s.

The above analysis assumes that soil moisture is available for evaporation during the entire period of soil aeration, and that the vapor pressure of the water in the soil is equal to that of bulk water. In fact, the vapor pressure of water is reduced somewhat when the water is evaporating from small capillaries with water-wettable walls, as seen from the Kelvin equation, so the vapor pressures of soil water are expected to be a little lower than those calculated by Eq. (75). Also, bound or adsorbed water is left out of the calculation, and it is assumed that the relative humidity of the water leaving the soil is 100%. And we presume that the contribution from soil thermal conductivity can be neglected. All of these approximations are such as to increase the magnitude of evaporative cooling above its true value, so our calculation provides an upper bound to the effect.

A program was written to integrate Eq. (76) numerically, and runs were made until steady-state soil temperatures were achieved. The parameters used are given in Table 3, and a plot of steady-state soil temperature versus initial air temperature is shown in Fig. 16. The amount of water evaporated from 1.6 kg of soil (1.0 L) during the time required to reach steady state ranged from 23.31 g (0°C initial air temperature) to 33.87 g (40°C initial air temperature). Evidently if the soil moisture content is greater than about 2%, one has sufficient water to reach the steady-state temperature. The air volumes required to reach steady state ranged from 3100 L (40°C) to 5300 L (0°C); recall that the size of the soil sample is 1.0 L. For all the runs presented here, the initial relative humidity was taken as zero.

Actually, for the bulk of the soil vapor stripping runs modeled, contaminant removal was essentially complete long before the steady-state soil temperature would have been achieved. The volume of the zone of influence used for the runs plotted in Fig. 12 is $\pi \times 20^2 \times 15 = 18{,}850$ m^3. The molar gas flow rates were about 9 mol/s, and roughly 2×10^6 s was required to bring about 99.99% removal. The volume of air used was therefore about 4.3×10^5 m^3, so the air volume/soil volume ratio is 23. (The parameters used for these runs were taken to simulate pilot runs at an actual soil vapor stripping site.) The ratios required to reach steady-state temperatures ranged from 3100 to 5300, over two orders of magnitude larger than those needed to achieve virtually complete removal of contaminant. A set of runs was therefore made in which the soil temperature was determined after 50 L of air had been passed through a 1-L soil sample. The resulting changes in soil temperature ranged from $-1.52°$ (initial air temperature = 0°C) to $+0.16°$ (initial air

TABLE 3
Model Parameters for Evaporative Cooling in Soil Vapor Stripping

Soil volume	1000 mL
Soil density	1.6 g/mL
Soil specific heat	0.2 cal/g · deg
Initial soil temperature	12.8°C
Latent heat of vaporization of water	540 cal/g

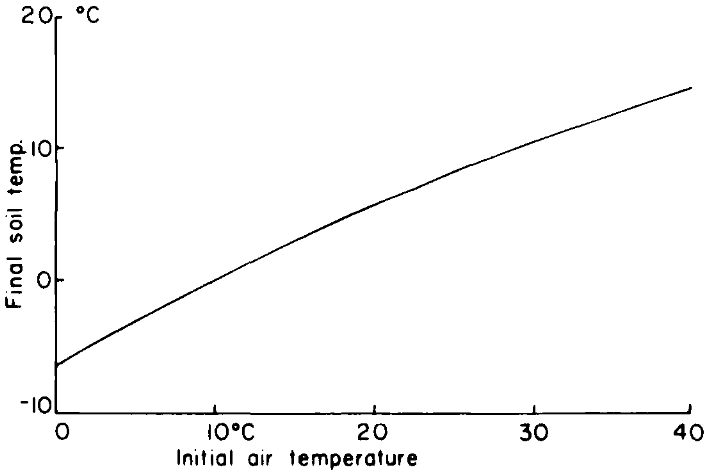

FIG. 16. Plot of steady-state soil temperature versus initial air temperature. The parameters for these runs and those in Fig. 17 are given in Table 3.

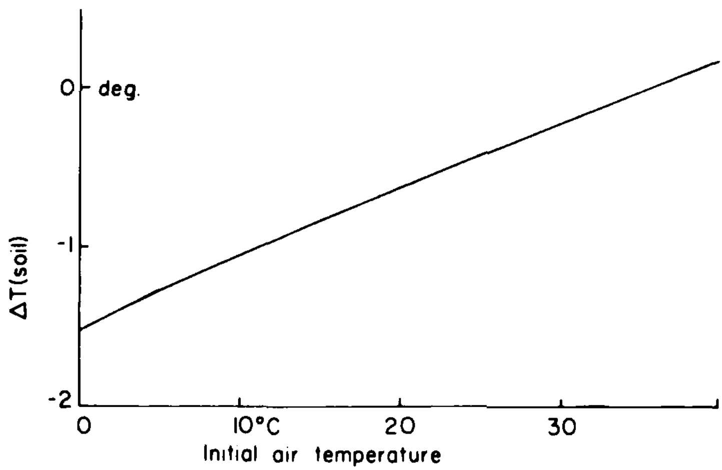

FIG. 17. Change in soil temperature after 50 volumes of air have been passed through 1 volume of soil as a function of initial air temperature. Parameters are given in Table 3.

temperature = 40°C). These are plotted in Fig. 17. These runs were made with an initial relative humidity of the air of zero; the temperature changes calculated are therefore larger than would occur with humid air.

We conclude that for most cases the temperature drop caused by evaporation of soil moisture will be no more than a degree or so. If long periods of aeration are required, steady-state soil temperatures may be quite substantially below the initial air temperature due to evaporation. Such cases, involving the vapor stripping of relatively nonvolatile compounds, are not likely to be economically practical because of the costs of pumping such large quantities of air.

CONCLUSIONS

The following conclusions can be drawn from our results:

(1) Use of impermeable circular caps to direct soil gas flow can increase overall vapor stripping removal rates by the order of 50%.
(2) Use of impermeable circular caps reduces somewhat the inefficiency of wells not drilled down nearly to the water table.
(3) Very long times are required for vapor stripping clean up if the radius of the zone of influence is much larger than the depth of the well. The radius of the zone of influence is about half the spacing between wells if they are laid out on a hexagonal grid (i.e., each well has six nearest neighbors).
(4) The effects of numerical dispersion, a mathematical artifact associated with the representation of advection terms by finite differences, do not appear to be significant in this model.
(5) The deleterious effect of low soil permeability may be compensated for, within practical limits, by increasing the radius of the gravel packing of the screened portion of the well. Gas flow rates are proportional to the product of this radius and the soil permeability.
(6) Under normal circumstances, evaporative cooling of soil during vapor stripping is expected to be less than 1.5°C below the initial soil temperature.

Acknowledgments

Dr. Wilson and Mr. Gannon are indebted to AWARE, Inc. (now Eckenfelder, Inc.), and to the Water Resources Research Center of the University of Tennessee for grants in support of this work.

REFERENCES

1. J. H. Clarke and R. D. Mutch Jr., "An Overview of *in Situ* Management Technologies Including Innovative Approaches," in *Proc. 2nd Annu. Hazardous Materials Conf. West,* Long Beach, California, December 3-5, 1986, pp. 110-123.
2. G. R. Brubaker and E. L. Crockett, "*In Situ* Aquifer Remediation Using Enhanced Bioreclamation," in *Proc. 4th Annu. Hazardous Materials Conf.,* Atlantic City, New Jersey, June 2-4, 1986, pp. 13-19.
3. W. E. Ellis, J. R. Payne, and G. D. McNabb, *Treatment of Contaminated Soils with Aqueous Surfactants,* U.S. EPA Report No. EPA/600/2-85/129, PB 86-122561.
4. J. H. Nash, *Field Studies of In Situ Soil Washing,* U.S. EPA Report EPA/600/2-87/110, PB88-146808, 1987.
5. A. N. Clarke, *Zone I Soil Decontamination through in Situ Vapor Stripping Processes,* Contract 68-02-4446, Final Report to EPA, AWARE, Inc., April 1987.
6. W. L. Wootan Jr. and T. Voynick, *Forced Venting to Remove Gasoline Vapor from a Large-Scale Aquifer,* Submitted by Texas Research Institute to American Petroleum Institute, Washington, D.C., January 13, 1984.
7. Woodard-Clyde Consultants, *Performance Evaluation Pilot Scale Installation and Operation, Soil Installation and Operation, Soil Gas Vapor Extraction System, Time Oil Company site, Tacoma, Washington, South Tacoma Channel, Well 12A Project,* Work Assignment 74-0N14.1, Walnut Creek, CA, Dec. 13, 1985.
8. G. J. Anastos, P. J. Parks, M. H. Corbin, and M. F. Coia, *In Situ Air Stripping of Soils Pilot Study,* Submitted by Roy F. Weston, Inc., to U.S. Army Toxic and Hazardous Materials AGency, Aberdeen Proving Ground, Maryland, October 1985, Report AMXTH-TE-TR-85026.
9. W. L. Crow, E. P. Anderson, and E. Minugh, *Subsurface Venting of Hydrocarbon Vapors from an Underground Aquifer,* Submitted by Riedel Environmental Services Co. and Radian Corp. to American Petroleum Institute, Washington, D.C., API Publication No. 4410, 1985.
10. D. J. Wilson, A. N. Clarke, and J. H. Clarke, *Sep. Sci. Technol., 23,* 991 (1988).
11. F. S. Shaw, *An Introduction to Relaxation Methods,* Dover, New York, 1953.
12. K. Gannon, Doctoral Dissertation, Vanderbilt University, 1988.
13. B. P. Leonard, "A Survey of Finite Differences of Opinion on Numerical Muddling of the Incomprehensible Defective Confusion Equation," in *Finite Element Methods for Convection Dominated Flows* (T. J. R. Hughes, ed.), American Society of Mechanical Engineers, New York, 1979, pp. 1-17.

Received by editor November 21, 1988